Dalton Transactions

COMMUNICATION

View Article Online
View Journal | View Issue

Cite this: *Dalton Trans.*, 2019, **48**, 12812

Received 28th March 2019,
Accepted 23rd July 2019

DOI: 10.1039/c9dt01319a

rsc.li/dalton

CO_2 hydrogenation by phosphorus–nitrogen PN^3P-pincer iridium hydride complexes: elucidation of the deactivation pathway†

Yupeng Pan,[a,b] Chao Guan,[a] Huaifeng Li,[a] Priyanka Chakraborty,[a] Chunhui Zhou[a] and Kuo-Wei Huang *[a]

PN^3P–Ir pincer hydride complexes were synthesized and characterized as catalysts and key intermediates in the direct hydrogenation of CO_2 to formate under mild conditions. The formation of a dearomatized PN^3P^*–Ir(I)–CO species was identified as a plausible key process accountable for the loss of catalytic activity in the CO_2 hydrogenation.

Carbon capture and sequestration (CCS) has been the subject of extensive research and commercial efforts.[1–5] The selective hydrogenation of carbon dioxide (CO_2) under mild conditions represents an economical and sustainable method of preparing valuable products and fuels from CO_2.[6,7] In this regard, significant achievements have been made using single-site homogeneous catalysts in CO_2 transformation, especially in the selective conversion of CO_2 and H_2 to formic acid or formate.[8,9] While the hydrogenation of CO_2 to HCOOH is thermodynamically favored in the aqueous phase, the energy barrier is high. As a result, high reaction pressures and temperatures are generally needed. A number of transition-metal complexes, such as rhodium,[10–15] ruthenium[16–27] and iridium,[28–37] have been investigated for the hydrogenation of CO_2. Among these metals, iridium complexes appear very promising.

In recent years, highly efficient and selective hydrogen transfer reactions and dehydrogenation reactions mediated by pincer-ligated complexes have been reported.[38,39] In addition, the catalytic conversion of *n*-alkanes to alkylaromatics using pincer supported iridium complexes[40–44] and of glycerol to lactic acid[45–47] have been well developed. For the reduction of CO_2, Himeda and Fujita *et al.* used a dinuclear proton-switchable iridium catalyst bearing an N,N′-type ligand, 4,4′,6,6′-tetrahydroxy-2,2′-bipyrimidine, as a bridging group, to afford an average TOF of 53 800 h^{-1} in the presence of $KHCO_3$ at 80 °C under 50 bar.[32] When a strong electron-donating PNP ligand was introduced into the CO_2 hydrogenation, high activities of Ir(III) complexes towards CO_2 hydrogenation were demonstrated by the Nozaki group (Fig. 1), and an unprecedentedly high TON of 3 500 000 was achieved.[29] Analogous "saturated" systems by Hazari *et al.* also showed a high TON of 348 000,[30] although a much higher temperature and pressure were necessary. Recent mechanistic studies on homogeneous iridium catalytic systems in CO_2 hydrogenation suggested that the CO_2 activation pathways are dependent on the nature of the Ir catalysts and that a hydrido ligand on an Ir(III) center is essential.[48–51]

We recently demonstrated that $PN^3(P)$-pincer complexes show unique properties in various challenging transformations in organic synthesis and catalytic studies,[52–57] showing diverse catalytic activities and different thermodynamic and kinetic properties.[58,59] Driven by the potential advantages of employing more electron-rich pincer complexes, herein, we present our development on PN^3P–Ir(III) trihydride complexes in CO_2 hydrogenation to formate. A probable catalyst-deactivation step in the formation of a dearomatized PN^3P^*Ir–CO complex is also discussed.

As has been suggested that Ir(III) trihydride complexes serve as effective catalysts in the hydrogenation of CO_2,[29] we devel-

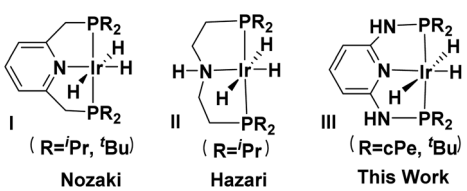

Fig. 1 Examples of PN^XP pincer Ir(III) trihydride catalysts for CO_2 hydrogenation.

[a]*KAUST Catalysis Center and Division of Physical Sciences and Engineering, King Abdullah University of Science and Technology, Thuwal 23955-6900, Saudi Arabia. E-mail: hkw@kaust.edu.sa*
[b]*Shenzhen Grubbs Institute, Southern University of Science and Technology (SUSTech), Shenzhen, 518055, P. R. China*

†Electronic supplementary information (ESI) available: Experimental procedures, characterization data, and ^1H and ^{13}C NMR spectra for the compounds. CCDC 1423984 (**4a**), 1423985 (**2b**), 1482628 (**5b**) and 1914804 (**3b**). For ESI and crystallographic data in CIF or other electronic format see DOI: 10.1039/c9dt01319a

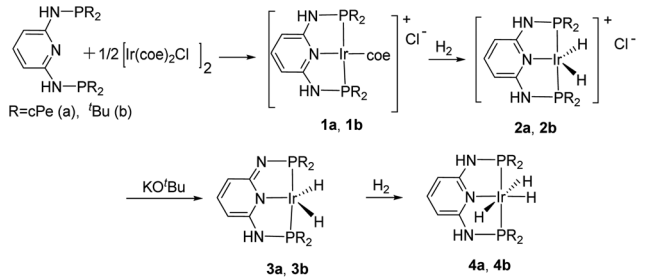

Scheme 1 Synthesis of PN^3P–Ir(III) trihydride complexes.

oped a general route for the synthesis of the Ir(III) complexes based on PN^3P ligands (Scheme 1). Cationic iridium(I) complexes **1a** and **1b** were synthesized by coordinating the PN^3PR ligands (R = cyclopentyl (cPe) and *t*-butyl (^{t}Bu)) with a stoichiometric amount of $[Ir(coe)_2Cl]_2$, similar to the procedure provided in the literature.[60] We then introduced H_2 to eliminate the coordinating coe moiety resulting in the formation of cationic iridium(III) complexes **2a** and **2b** after the oxidative addition of one equivalent of H_2. The NMR data of **2b** collected in $CDCl_3$ at room temperature showed only one N–H (2H, δ 9.27 ppm) signal and one Ir–H (2H, δ −26.87 ppm) signal in the ^{1}H NMR spectrum and a signal at δ 126.2 ppm in the ^{31}P NMR spectrum, suggesting a symmetric conformation enforced by the PN^3P pincer ligand. In addition, the solid state molecular structure of **2b** was consistent with the NMR details where two hydrides are equivalent (Fig. 2). The structure shows a square pyramidal configuration with a chloride as a dissociated counter anion.

The neutral dearomatized complexes **3a** and **3b** were obtained by employing one equivalent of KO^{t}Bu to deprotonate one of the NH arms in the PN^3P pincer ligand.[61,62] Unlike their –CH_2 analogs,[62] these dearomatized PN^3P^* complexes were stable enough to be isolated at room temperature. The ^{1}H NMR spectrum of **3b** in C_6D_6 shows three sets of sp^2 C–H signals at δ 5.21 (d), 6.85 (d), and 6.92 (t) ppm, in agreement with the dearomatization of the central pyridine ring. As expected, two sets of doublet phosphorus signals were observed in the ^{31}P NMR spectrum ($^2J_{P-P}$ = 299 Hz), with an apparent triplet for a hydride ($^2J_{P-H}$ = 12.0 Hz) at δ −24.93 ppm in the ^{1}H NMR spectrum.[38,52–56,58,59] The solid-state molecular structure of **3b** was obtained with two peaks in the Fourier map, indicative of two hydrides forming a distorted trigonal bipyramidal configuration (Fig. 3).

Finally, the trihydride complexes **4a** and **4b** were obtained by treating **3a** and **3b** in the presence of H_2 in THF. The ^{1}H NMR spectrum of complex **4a** in C_6D_6 shows two sets of hydride signals, at δ −18.15 ppm and −11.76 ppm with an integral intensity ratio of 2 : 1, and two sets of signals for three protons in the sp^2 region (5.60 (d) and 6.81 (t) ppm), indicating the rearomatization of the central pyridine ring. Complex **4a** was confirmed by the X-ray diffraction analysis (Fig. 4). The solid-state molecular structure of **4a** was consistent with the NMR details. Trihydride **4a** has an octahedral geometry with three peaks in the Fourier map assigned to hydrides on the Ir center, consistent with the reported ^{i}Pr–PNP–Ir trihydride compound.[29]

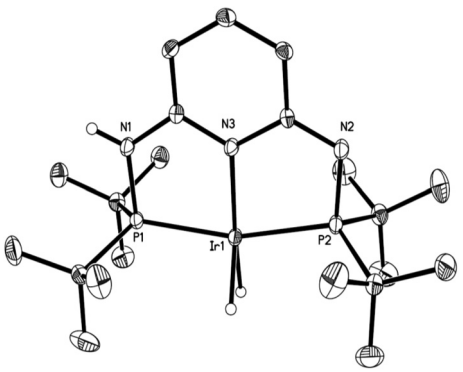

Fig. 3 X-ray structure of complex **3b** with 40% probability of thermal ellipsoids. The solvent and hydrogen atoms, except N–H and hydrides, were omitted for clarity. Selected bond lengths (Å): (**3b**) Ir1–N3 2.063(6), Ir1–P1 2.2725(8), and Ir1–P2 2.2955(8). Selected bond angles (°): (**3b**) P1–Ir1–P2 162.79(3).

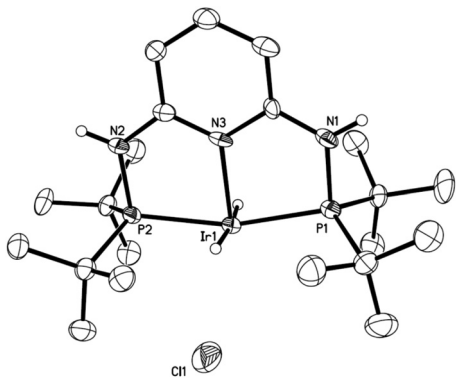

Fig. 2 X-ray structure of complex **2b** with 40% probability of thermal ellipsoids. The solvent and hydrogen atoms, except N–H and hydrides, were omitted for clarity. Selected bond lengths (Å): Ir1–N3 2.110(6), Ir1–P1 2.284(2), and Ir1–P2 2.279(2). Selected bond angles (°): (**2b**) P1–Ir1–P2 163.64(7).

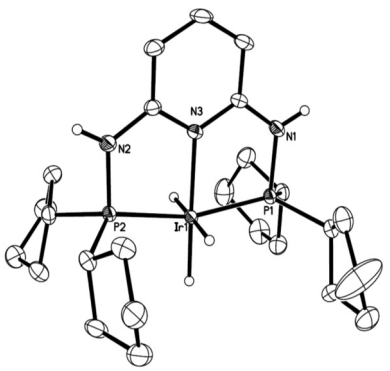

Fig. 4 X-ray structures of complex **4a** with 40% probability of thermal ellipsoids. The solvent and hydrogen atoms, except N–H and hydrides, were omitted for clarity. Selected bond lengths (Å): (**4a**) Ir1–N3 2.117(3). Selected bond angles (°): (**4a**) P1–Ir1–P2 164.07(3).

Several pincer-ligated iridium hydride complexes[29,30] are well known to catalyze CO_2 hydrogenation. Therefore, the catalytic activity of complexes **4a** and **4b** was examined accordingly in THF/H_2O solution (Table 1). According to the results of entries 1 and 2, the performance of **4b** (yield 17.6%) is better than that of **4a** (yield 6.3%) under the same conditions. **4b** was thus chosen to evaluate the influence of the reaction conditions, such as temperature and reaction time, for the CO_2 hydrogenation reaction. The results of entries 2–4 show that the yield increases (17.6% to 49.6%) in the beginning with increasing temperature (120–130 °C), but then decreases with temperature increasing continually (130–140 °C). These observations suggest that **4b** is not stable at high temperature. Prolonging the reaction time to 18 hours did not improve the yield of formate (49.6% to 51.0%, entry 5), indicating that **4b** is likely to be deactivated within 12 hours.

To gain more insight into the catalyst deactivation, additional experiments were carried out. The treatment of **4b** with H_2 and CO_2 (1 : 1, 120 psi) at 140 °C for 24 hours afforded **5b** in 78% yield after recrystallization (Scheme 2), and in this process, the water should be generated as a by-product (Scheme 2). Furthermore, the hydrogenation of CO_2 which is catalyzed by complex **5b** showed no activity (Table 1, entry 6). The ^{31}P NMR spectrum of **5b** indicated the presence of two nonequivalent P atoms. In the ^1H NMR spectrum, three sets of sp^2 C–H signals at 5.11(d), 6.74 (d), and 6.83 (t) ppm were observed, indicating the dearomatization of the central pyridine ring. The molecular structure of **5b** shows a slightly distorted square-planar coordination geometry (Fig. 5). The metal–carbon bond distance is 1.837(6) Å, just slightly longer than that in the PNP–Ir–CO complex (Ir–CO: 1.818(2) Å).[62] The Ir–N bond distance of **5b** (2.076(4) Å) and that in the PNP–Ir–CO complex (2.083(2) Å) were practically identical. Consistent with our results, **5b** was unable to catalyze the CO_2 hydrogenation under the same conditions shown in Table 1. The formation of the CO ligand implies that the reverse water gas shift (RWGS) reaction also takes place in the presence of the PN^3P–Ir complex,[62–66] and this process is likely responsible for the loss of catalytic activity.

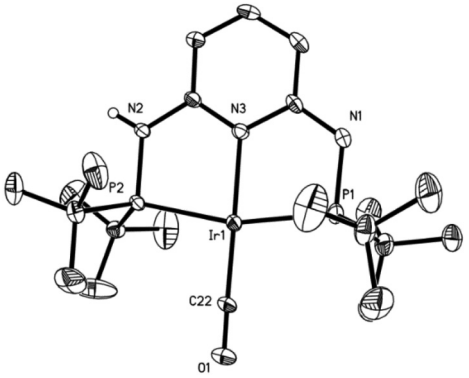

Fig. 5 X-ray structure of **5b** with 40% probability of thermal ellipsoids. The solvent and hydrogen atoms, except N–H, were omitted for clarity. Selected bond lengths (Å): (**5b**) Ir1–N3 2.076(4), Ir1–C22 1.837(6), Ir1–P1 2.3000(14), and Ir1–P2 2.3008(13). Selected bond angles (°): (**5b**) P1–Ir1–P2 163.33(5) and C(22)–Ir(1)–N(1) 179.3(2).

Table 1 Hydrogenation of CO_2 catalyzed by Ir(III)-pincer complexes

Entry	Cat.	T (°C)	P (psi)	Time (h)	Yield[a] (%)	TON	TOF (h^{-1})
1	**4a**	120	120	12	6.3	630	53
2	**4b**	120	120	12	17.6	1760	147
3	**4b**	130	120	12	49.6	4960	413
4	**4b**	140	120	12	30.6	3060	255
5	**4b**	130	120	18	51.0	5100	283
6	**5b**	130	120	18	—	—	—

[a] Total pressure at room temperature: 120 psi ($H_2 : CO_2$ = 1 : 1). Yields: Calculated by ^1H NMR analysis using sodium 3-(trimethylsilyl)-1-propanesulfonate as an internal standard, based on the added KOH base (1.0×10^{-3} mol). Catalyst loading: 1.0×10^{-7} mol. [THF]/[H_2O] = 1/4 (ratio by volume).

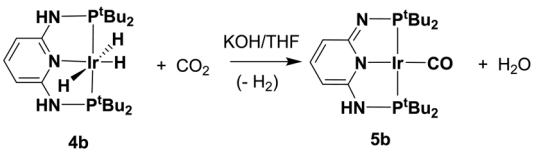

Scheme 2 Production complex **5b** from complex **4b** in the presence of CO_2/H_2.

In summary, we have developed a general method for synthesizing PN^3P pincer Ir(III) trihydride complexes and obtained several key structures involved in the CO_2 hydrogenation process. While the Ir complexes showed favorable activity (a turnover number up to 5100), the formation of a dearomatized PN^3P^*–Ir(I)–CO species was identified as a plausible key pathway for the catalyst deactivation. Our work reveals that the RWGS should be taken into account for future catalyst design to avoid this unfavorable process to maximize the catalyst activity and lifetime.

Conflicts of interest

There are no conflicts to declare.

Acknowledgements

This work was supported by funding from the King Abdullah University of Science and Technology (KAUST).

Notes and references

1 P. G. Jessop, F. Joó and C.-C. Tai, *Coord. Chem. Rev.*, 2004, **248**, 2425.
2 T. Sakakura, J.-C. Choi and H. Yasuda, *Chem. Rev.*, 2007, **107**, 2365.
3 C. Gunanathan and D. Milstein, *Chem. Rev.*, 2014, **114**, 12024.

4 J. Artz, T. E. Müller, K. Thenert, J. Kleinekorte, R. Meys, A. Sternberg, A. Bardow and W. Leitner, *Chem. Rev.*, 2017, **118**, 434.
5 M. Bui, C. S. Adjiman, A. Bardow, E. J. Anthony, A. Boston, S. Brown, P. S. Fennell, S. Fuss, A. Galindo and L. A. Hackett, *Energy Environ. Sci.*, 2018, **11**, 1062.
6 M. Aresta, *Carbon dioxide as chemical feedstock*, John Wiley & Sons, 2010.
7 M. Cokoja, C. Bruckmeier, B. Rieger, W. A. Herrmann and F. E. Kühn, *Angew. Chem., Int. Ed.*, 2011, **50**, 8510.
8 S. Moret, P. J. Dyson and G. Laurenczy, *Nat. Commun.*, 2014, **5**, 4017.
9 K. Sordakis, C. Tang, L. K. Vogt, H. Junge, P. J. Dyson, M. Beller and G. Laurenczy, *Chem. Rev.*, 2017, **118**, 372.
10 J. C. Tsai and K. M. Nicholas, *J. Am. Chem. Soc.*, 1992, **114**, 5117.
11 T. Burgemeister, F. Kastner and W. Leitner, *Angew. Chem., Int. Ed. Engl.*, 1993, **32**, 739.
12 F. Gassner and W. Leitner, *J. Chem. Soc., Chem. Commun.*, 1993, **19**, 1465.
13 W. Leitner, E. Dinjus and F. Gaßner, *J. Organomet. Chem.*, 1994, **475**, 257.
14 R. Fornika, H. Gorls, B. Seemann and W. Leitner, *J. Chem. Soc., Chem. Commun.*, 1995, **14**, 1479.
15 Y.-N. Li, L.-N. He, A.-H. Liu, X.-D. Lang, Z.-Z. Yang, B. Yu and C.-R. Luan, *Green Chem.*, 2013, **15**, 2825.
16 P. G. Jessop, T. Ikariya and R. Noyori, *Nature*, 1994, **368**, 231.
17 P. G. Jessop, Y. Hsiao, T. Ikariya and R. Noyori, *J. Am. Chem. Soc.*, 1996, **118**, 344.
18 C. Yin, Z. Xu, S.-Y. Yang, S. M. Ng, K. Y. Wong, Z. Lin and C. P. Lau, *Organometallics*, 2001, **20**, 1216.
19 P. Munshi, A. D. Main, J. C. Linehan, C.-C. Tai and P. G. Jessop, *J. Am. Chem. Soc.*, 2002, **124**, 7963.
20 J. Elek, L. Nádasdi, G. Papp, G. Laurenczy and F. Joó, *Appl. Catal., A*, 2003, **255**, 59.
21 C. Federsel, R. Jackstell, A. Boddien, G. Laurenczy and M. Beller, *ChemSusChem*, 2010, **3**, 1048.
22 G. A. Filonenko, R. van Putten, E. N. Schulpen, E. J. Hensen and E. A. Pidko, *ChemCatChem*, 2014, **6**, 1526.
23 J. Kothandaraman, M. Czaun, A. Goeppert, R. Haiges, J. P. Jones, R. B. May, G. S. Prakash and G. A. Olah, *ChemSusChem*, 2015, **8**, 1442.
24 K. Rohmann, J. Kothe, M. W. Haenel, U. Englert, M. Hölscher and W. Leitner, *Angew. Chem., Int. Ed.*, 2016, **55**, 8966.
25 G. H. Gunasekar, J. Shin, K.-D. Jung, K. Park and S. Yoon, *ACS Catal.*, 2018, **8**, 4346.
26 P. Hu, Y. Ben-David and D. Milstein, *Angew. Chem., Int. Ed.*, 2016, **55**, 1061.
27 C. Guan, Y. Pan, E. P. L. Ang, J. Hu, C. Yao, M.-H. Huang, H. Li, Z. Lai and K.-W. Huang, *Green Chem.*, 2018, **20**, 4201.
28 Y. Himeda, N. Onozawa-Komatsuzaki, H. Sugihara and K. Kasuga, *Organometallics*, 2007, **26**, 702.
29 R. Tanaka, M. Yamashita and K. Nozaki, *J. Am. Chem. Soc.*, 2009, **131**, 14168.
30 T. J. Schmeier, G. E. Dobereiner, R. H. Crabtree and N. Hazari, *J. Am. Chem. Soc.*, 2011, **133**, 9274.
31 R. Tanaka, M. Yamashita, L. W. Chung, K. Morokuma and K. Nozaki, *Organometallics*, 2011, **30**, 6742.
32 J. F. Hull, Y. Himeda, W.-H. Wang, B. Hashiguchi, R. Periana, D. J. Szalda, J. T. Muckerman and E. Fujita, *Nat. Chem.*, 2012, **4**, 383.
33 W.-H. Wang, J. F. Hull, J. T. Muckerman, E. Fujita and Y. Himeda, *Energy Environ. Sci.*, 2012, **5**, 7923.
34 W.-H. Wang, J. T. Muckerman, E. Fujita and Y. Himeda, *ACS Catal.*, 2013, **3**, 856.
35 S. Xu, N. Onishi, A. Tsurusaki, Y. Manaka, W. H. Wang, J. T. Muckerman, E. Fujita and Y. Himeda, *Eur. J. Inorg. Chem.*, 2015, **2015**, 5591.
36 R. Puerta-Oteo, M. Hölscher, M. V. Jiménez, W. Leitner, V. Passarelli and J. s. J. Pérez-Torrente, *Organometallics*, 2017, **37**, 684.
37 Z. Lu, V. Cherepakhin, I. Demianets, P. J. Lauridsen and T. Williams, *Chem. Commun.*, 2018, **54**, 7711.
38 H. Li, B. Zheng and K.-W. Huang, *Coord. Chem. Rev.*, 2015, **293–294**, 116.
39 H. Li, T. P. Gonçalves, D. Lupp and K.-W. Huang, *ACS Catal.*, 2019, **9**, 1619.
40 J. Choi, A. H. R. MacArthur, M. Brookhart and A. S. Goldman, *Chem. Rev.*, 2011, **111**, 1761.
41 M. C. Haibach, S. Kundu, M. Brookhart and A. S. Goldman, *Acc. Chem. Res.*, 2012, **45**, 947.
42 C. Cheng, B. G. Kim, D. Guironnet, M. Brookhart, C. Guan, D. Y. Wang, K. Krogh-Jespersen and A. S. Goldman, *J. Am. Chem. Soc.*, 2014, **136**, 6672.
43 M. C. Haibach, N. Lease and A. S. Goldman, *Angew. Chem., Int. Ed.*, 2014, **53**, 10160.
44 S. Fang, H. Chen and H. Wei, *RSC Adv.*, 2018, **8**, 9232.
45 J. Campos, U. Hintermair, T. P. Brewster, M. K. Takase and R. H. Crabtree, *ACS Catal.*, 2014, **4**, 973.
46 L. S. Sharninghausen, J. Campos, M. G. Manas and R. H. Crabtree, *Nat. Chem.*, 2014, **5**, 973.
47 M. Iglesias and L. A. Oro, *Chem. Soc. Rev.*, 2018, **47**, 2772.
48 A. Azua, S. Sanz and E. Peris, *Chem. – Eur. J.*, 2011, **17**, 3963.
49 F. J. Fernández-Alvarez, M. Iglesias, L. A. Oro and V. Polo, *ChemCatChem*, 2013, **5**, 3481.
50 Y. Suna, M. Z. Ertem, W.-H. Wang, H. Kambayashi, Y. Manaka, J. T. Muckerman, E. Fujita and Y. Himeda, *Organometallics*, 2014, **33**, 6519.
51 Y. Suna, Y. Himeda, E. Fujita, J. T. Muckerman and M. Z. Ertem, *ChemSusChem*, 2017, **10**, 4535.
52 T. Chen, L.-P. He, D. Gong, L. Yang, X. Miao, J. Eppinger and K.-W. Huang, *Tetrahedron Lett.*, 2012, **53**, 4409.
53 L.-P. He, T. Chen, D. Gong, Z. Lai and K.-W. Huang, *Organometallics*, 2012, **31**, 5208.
54 L.-P. He, T. Chen, D.-X. Xue, M. Eddaoudi and K.-W. Huang, *J. Organomet. Chem.*, 2012, **700**, 202.
55 T. Chen, H. Li, S. Qu, B. Zheng, L. He, Z. Lai, Z.-X. Wang and K.-W. Huang, *Organometallics*, 2014, **33**, 4152.
56 D. Gong, W. Liu, T. Chen, Z.-R. Chen and K.-W. Huang, *J. Mol. Catal. A: Chem.*, 2014, **395**, 100.

57 H. Li, Y. Wang, Z. Lai and K.-W. Huang, *ACS Catal.*, 2017, **7**, 4446.
58 Y. Wang, B. Zheng, Y. Pan, C. Pan, L. He and K.-W. Huang, *Dalton Trans.*, 2015, **44**, 15111.
59 Y. Pan, C. L. Pan, Y. Zhang, H. Li, S. Min, X. Guo, B. Zheng, H. Chen, A. Anders, Z. Lai and K.-W. Huang, *Chem. – Asian J.*, 2016, **11**, 1357.
60 C. Zhou, J. Hu, Y. Wang, C. Yao, P. Chakraborty, H. Li, C. Guan, M.-H. Huang and K.-W. Huang, *Org. Chem. Front.*, 2019, **6**, 721.
61 M. Gupta, C. Hagen, W. C. Kaska, R. E. Cramer and C. M. Jensen, *J. Am. Chem. Soc.*, 1997, **119**, 840.
62 M. Feller, U. Gellrich, A. Anaby, Y. Diskin-Posner and D. Milstein, *J. Am. Chem. Soc.*, 2016, **138**, 6445.
63 A. Anaby, M. Feller, Y. Ben-David, G. Leitus, Y. Diskin-Posner, L. J. Shimon and D. Milstein, *J. Am. Chem. Soc.*, 2016, **138**, 9941.
64 W. C. Kaska, S. Nemeh, A. Shirazi and S. Potuznik, *Organometallics*, 1988, **7**, 13.
65 S. Nemeh, C. Jensen, E. Binamira-Soriaga and W. C. Kaska, *Organometallics*, 1983, **2**, 1442.
66 K.-W. Huang, J. H. Han, C. B. Musgrave and E. Fujita, *Organometallics*, 2007, **26**, 508.